ADVANCED HEALTHCARE MATERIALS
www.advhealthmat.de

Targeted Therapy of Osteoarthritis via Intra-Articular Delivery of Lipid-Nanoparticle-Encapsulated Recombinant Human FGF18 mRNA

Mengze Sun, Bin Ma, Zihang Pan, Yun Zhao, Liangliang Tian, Yifei Fan, Weijing Kong, Junyan Wang, Boyang Xu, Yingfang Ao, Quanyi Guo, Xi Wang, Xiaohong Peng, Xiaoxia Li, Jin Cheng, Lei Miao,* Kai Wang,* and Xiaoqing Hu**

Fibroblast growth factor 18 (FGF18) emerges as a promising therapeutic target for osteoarthritis (OA). In this study, a novel articular cavity-localized lipid nanoparticle (LNP) named WG-PL14 is developed. This optimized formulation has a nearly 30-fold increase in mRNA expression as well as better articular cavity enrichment compared to commercial lipids MC3 when performing intra-articular injection. Then, a mRNA sequence encoding recombinant human FGF18 (rhFGF18) for potential mRNA therapy in OA is optimized. In vitro assays confirm the translation of rhFGF18 mRNA into functional proteins within rat and human chondrocytes, promoting cell proliferation and extracellular matrix (ECM) synthesis. Subsequently, the therapeutic efficacy of the LNP-rhFGF18 mRNA complex is systematically assessed in a mouse OA model. The administration exhibits several positive outcomes, including an improved pain response, upregulation of ECM-related genes (e.g., AGRN and HAS2), and remodeling of subchondral bone homeostasis compared to a control group. Taken together, these findings underscore the potential of localized LNP-rhFGF18 mRNA therapy in promoting the regeneration of cartilage tissue and mitigating the progression of OA.

1. Introduction

Osteoarthritis (OA) is the predominant form of arthritis and is marked by persistent joint pain and disability.[1] The rising age of the global population and the escalating prevalence of obesity are primary contributors to the continual growth in OA cases observed worldwide.[2] Apart from the substantial impact on individuals, the socioeconomic expenses associated with OA are significant. Consequently, OA emerges as a noteworthy public health challenge expected to persist in the coming decades. Addressing the multifaceted aspects of this condition is imperative to mitigate its individual and societal consequences.[3,4] Common clinical strategies for OA, such as lifestyle management, physical therapy, and medication, mainly aim at symptom relief rather than reversing the underlying disease processes. Thus, there is an ongoing need for research and development of interventions that can modify the course of OA and potentially offer disease-modifying effects.[5]

M. Sun, Y. Fan, J. Wang, B. Xu, Y. Ao, J. Cheng, X. Hu
Department of Sports Medicine
Institute of Sports Medicine of Peking University
Beijing Key Laboratory of Sports Injuries
Peking University Third Hospital
Beijing 100191, China
E-mail: chengjin@bjmu.edu.cn; huxiaoqingbd01@sina.com

The ORCID identification number(s) for the author(s) of this article can be found under https://doi.org/10.1002/adhm.202400804

© 2024 The Author(s). Advanced Healthcare Materials published by Wiley-VCH GmbH. This is an open access article under the terms of the Creative Commons Attribution-NonCommercial-NoDerivs License, which permits use and distribution in any medium, provided the original work is properly cited, the use is non-commercial and no modifications or adaptations are made.

DOI: 10.1002/adhm.202400804

M. Sun, Y. Fan, J. Wang, B. Xu, Y. Ao, J. Cheng, X. Hu
Engineering Research Center of Sports Trauma Treatment Technology and Devices
Ministry of Education
Beijing 100191, China

B. Ma, L. Miao
State Key Laboratory of Natural and Biomimetic Drugs
School of Pharmaceutical Sciences
Peking University
Beijing 100191, China
E-mail: lmiao_pharm@bjmu.edu.cn

B. Ma, L. Miao
Beijing Key Laboratory of Molecular Pharmaceutics
School of Pharmaceutical Sciences
Peking University
Beijing 100191, China

Fibroblast growth factor 18 (FGF18) belongs to the FGF8 subfamily, which can bind and activate FGFR3 signaling.[6] Notably, FGF18 exhibits protective roles in OA. By stimulating downstream signaling of MAPK, FGF18 plays a significant role in synovial joint development, stimulating the proliferation and accumulation of type II collagen and proteoglycans in cultured chondrocytes.[7,8] Additionally, it promotes chondrogenesis and cartilage repair in injury-induced rat models of OA, identifying FGF18 as a molecule protective against articular cartilage degeneration.[9] As a potential therapeutic target of OA, sprifermin, a recombinant human fibroblast growth factor 18 (rhFGF18), has been investigated as a potential disease-modifying OA drug.[10] Nevertheless, the prolonged and costly production of protein drugs has constrained their widespread application in clinical treatments.[11] This underscores the imperative to innovate and devise new delivery methods for rhFGF18.

To date, mRNA has emerged as a promising alternative for delivering therapeutic proteins.[12,13] Since the targeted protein is produced via translation by endogenous cells, mRNA facilitates post-translational modifications resembling endogenous proteins. In contrast to DNA or viral-based gene therapies, mRNA does not require nuclear localization, reducing the risks of genomic insertions and mutations. Crucially, mRNA therapy allows transient expression with a defined half-life, avoiding constitutive gene expression which may bring several potential side effects.[14] These features position mRNA as a potential method for delivering proteins with complex biophysical properties, including growth factors.

Whereas, mRNA poses challenges for intracellular delivery due to its negative charge, which prevents it from crossing the anionic lipid bilayer of cell membranes. Additionally, mRNA is susceptible to degradation by nucleases present in the body. To overcome these hurdles, lipid nanoparticles (LNPs) are utilized, particularly those containing ionizable cationic lipids. The incorporation of ionizable cationic lipids in LNPs allows for electrostatic interactions with nucleic acids, enabling effective binding and condensation of the mRNA. This condensation process shields the mRNA from nuclease degradation. Furthermore, the LNPs can be internalized into cells through endocytic pathways, facilitating efficient in vivo mRNA delivery. Another notable advantage of using ionizable LNPs is their neutral charge at physiological pH. This characteristic makes them relatively safer when compared to conventional cationic lipids or polymers typically used for RNA condensation in vivo applications.[15–18] Nowadays, LNPs stand as the only FDA-approved nonviral delivery platform for mRNA therapeutics. Various new LNP formulations have undergone evaluation in preclinical settings. Nevertheless, achieving targeted delivery of the LNP-mRNA complex to specific tissues or organs remains a challenge. Current LNP formulations can be absorbed and drained into peripheral blood, regardless of whether systemic or localized injection is employed. The off-target LNPs will accumulate in the liver, causing potential toxicity. Consequently, a library screening of new LNP formulations was conducted to enable localized LNP delivery to the muscle for immune protection and to tumors for cancer therapy.[19,20] For OA treatments, targeted delivery via intra-articular injection is preferred due to the avascular nature of the articular cavity. Nowadays, to our best knowledge, the targeted delivery of the LNP-mRNA complex to the articular cavity has not yet been achieved. In this context, we design a new LNP formulation for localized delivery to joints to facilitate the in situ retention of rhFGF18 mRNA.

In this study, we propose a disease-modifying strategy for OA, emphasizing in situ mRNA delivery of rhFGF18, a therapeutic, cartilage-anabolic growth factor. We first propose the localized delivery of LNP to joint and screen out a new multiamine lipid from a lipid library composed of 1000 lipids. We also optimize the formulation to control the particle size and surface charge to facilitate the maintenance of the LNP-mRNA complex. The resulting LNP, WG-PL14, owns an almost 30-fold increase in mRNA expression as well as better enrichment in the articular cavity compared to commercial lipids MC3. Then we characterize the effect of rhFGF18 mRNA on primary rat chondrocytes, human normal, and OA chondrocytes, showing the ability of rhFGF18 to promote cell proliferation and ECM synthesis. At last, we evaluate the therapeutic potential of rhFGF18 in the mouse OA model, revealing the improved pain response and remodeling of subchondral bone homeostasis. Overall, these findings suggest that rhFGF18 mRNA is a novel therapeutic way for OA.

2. Results

2.1. Optimizing LNP Formulation for rhFGF18 mRNA Delivery

In our study, we selected PL14, a cationic ionizable lipid, from a novel ionizable lipid library called PAMA, with improved efficiency in delivering mRNA to the joint through intra-articular injection (**Figure** 1A). To establish our initial formulation, we employed compositions similar to lipidoids such as cKK-E12 and C12-200, which consist of ≈16 mol% phosphatidylethanolamine (DOPE) as a helper lipid and 2.5 mol% polyethylene glycol 2000 (PEG-2000) (Table S1, Supporting Information). However, we encountered issues with LNP leakage into the systemic circulation and mRNA expression in the liver.

To address these challenges and optimize the specific accumulation of LNPs and mRNA in the cartilage cavity, we made modifications to the original formulation by adjusting the water-to-ethanol ratio (W/O ratio), the N/P ratio, the percentage of PEG, and the dialysis buffer (Figure 1B). We observed a slight decrease in liver expression when we increased the N/P ratio of LNPs

Z. Pan, Y. Zhao, L. Tian, W. Kong, X. Peng, X. Li, K. Wang
Department of Physiology and Pathophysiology
School of Basic Medical Sciences
State Key Laboratory of Vascular Homeostasis and Remodeling
Peking University
Beijing 100191, China
E-mail: kai.wang88@pku.edu.cn
Q. Guo
Institute of Orthopedics
The Fourth Medical Center
Chinese PLA General Hospital
Beijing Key Lab of Regenerative Medicine in Orthopedics
Key Laboratory of Musculoskeletal Trauma & War Injuries PLA
No. 28 Fuxing Road, Haidian District, Beijing 100853, China
X. Wang
State Key Laboratory of Female Fertility Promotion
Clinical Stem Cell Research Center
Peking University Third Hospital
Beijing 100191, China

© 2024 The Author(s). Advanced Healthcare Materials published by Wiley-VCH GmbH

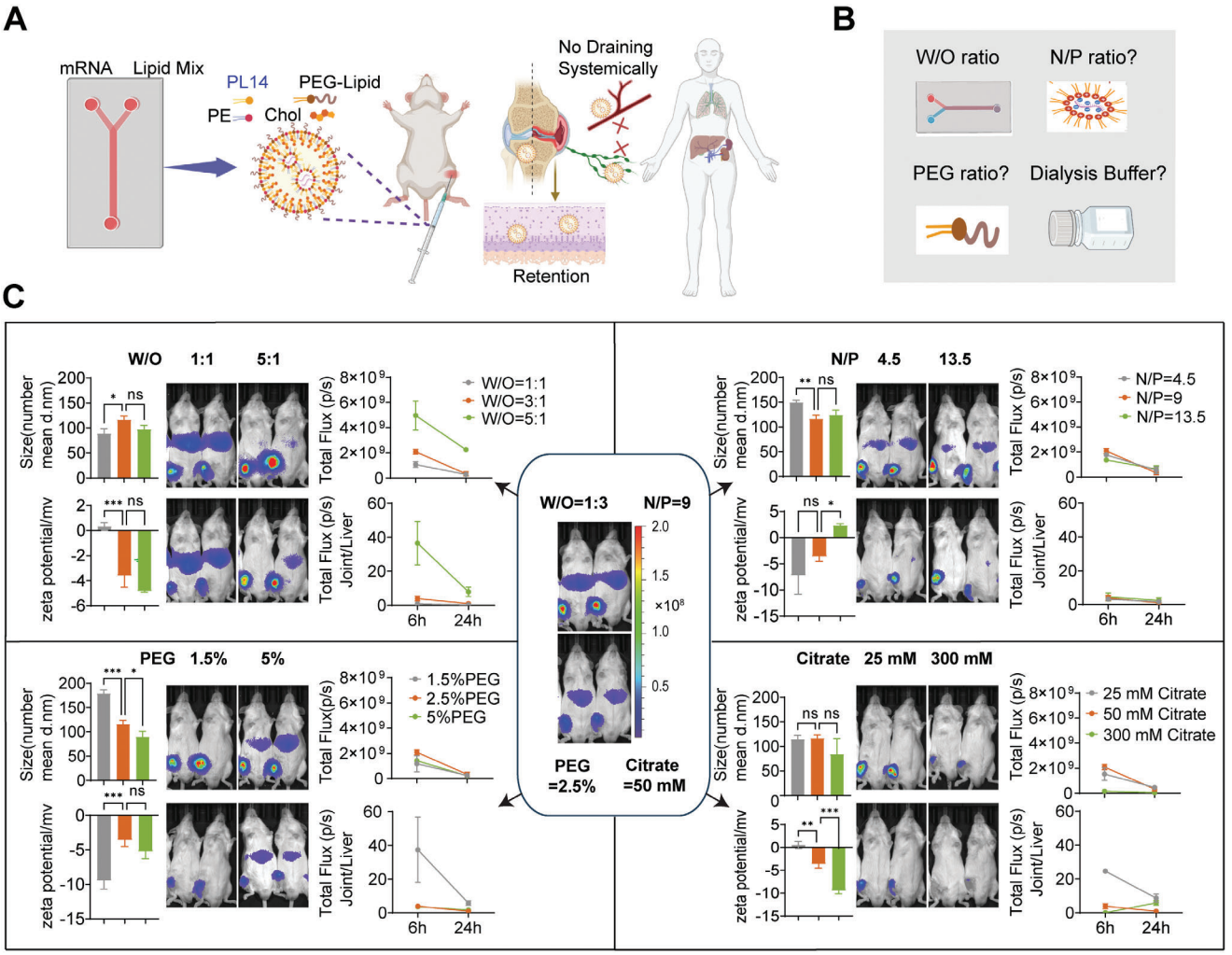

Figure 1. Formulation optimizations of PL14 LNPs to improve the specific accumulation of LNPs and mRNA in the articular cavity while minimizing expression in the liver. A) Schematic illustration of the preparation method of nanoparticles. B) Illustration of enhanced accumulation of Luc-mRNA LNPs in cartilage cavity by adjusting the water-to-ethanol ratio (W/O ratio), the N/P ratio, the percentage of PEG, and the concentration of dialysis buffer. C) The size, zeta potential, and bioluminescence images of ICR mice ($n = 3$) after intra-articular injection of LNP-Luc mRNA (2 μg mRNA) in different formulations. The unit of the fluorescent scale bar is photons/sec/cm^2/sr, the radiance scale of 1.0×10^7–2×10^8. Data were represented as mean ± SEM. Statistical significance was calculated via one-way ANOVA, followed by Dunnett's multiple comparisons test ($^*p < 0.05$, $^{**}p < 0.01$, and $^{***}p < 0.001$).

(Figure 1C). The incorporation of more ionizable cationic lipids resulted in a slight increase in the surface charge. To further evaluate whether increasing the charge density could improve the retention and expression of LNPs in cartilage, we formulated another cationic LNPs by incorporating the cationic lipid DOTAP into the WG-PL14 LNPs (refer to the work by Cheng et al for the DOTAP formulation).[21] However, despite observing the expression of most of the mRNA within the cartilage, the protein expression was not as high as without the addition of DOTAP (Figure S2C, Supporting Information). This suggests that mRNA expression is influenced by a combination of factors, including binding, cellular uptake, and endosomal release. Moreover, cationic lipids are often associated with increased inflammation.[22] Therefore, for local injections, we focused on LNPs with net neutral to negative charges to minimize potential inflammatory responses.

Notably, we discovered that increasing the W/O ratio and decreasing the PEG ratio, along with reducing surface charge and increasing particle size, resulted in significant improvements in LNP accumulation and mRNA expression within the cartilage cavity, while reducing systemic exposure (Figure 1C). This finding may seem counterintuitive; however, it aligns with previous reports indicating that smaller particles are more likely to be cleared by lymphatic drainage and systemic circulation. Thus, increasing particle size is one mechanism for achieving local particle expression.[23]

In addition to particle size, the type and amount of PEG play a crucial role in the uptake of LNPs by chondrocytes. Higher PEG amounts enhance surface hydrophilicity and inhibit local cellular uptake. Additionally, lower PEG alkyl chain lengths resulted in faster shedding.[24] To validate our choice of PEG-lipid, we further modified the PEG from C14-PEG to C18-PEG (DSG) and found

© 2024 The Author(s). Advanced Healthcare Materials published by Wiley-VCH GmbH

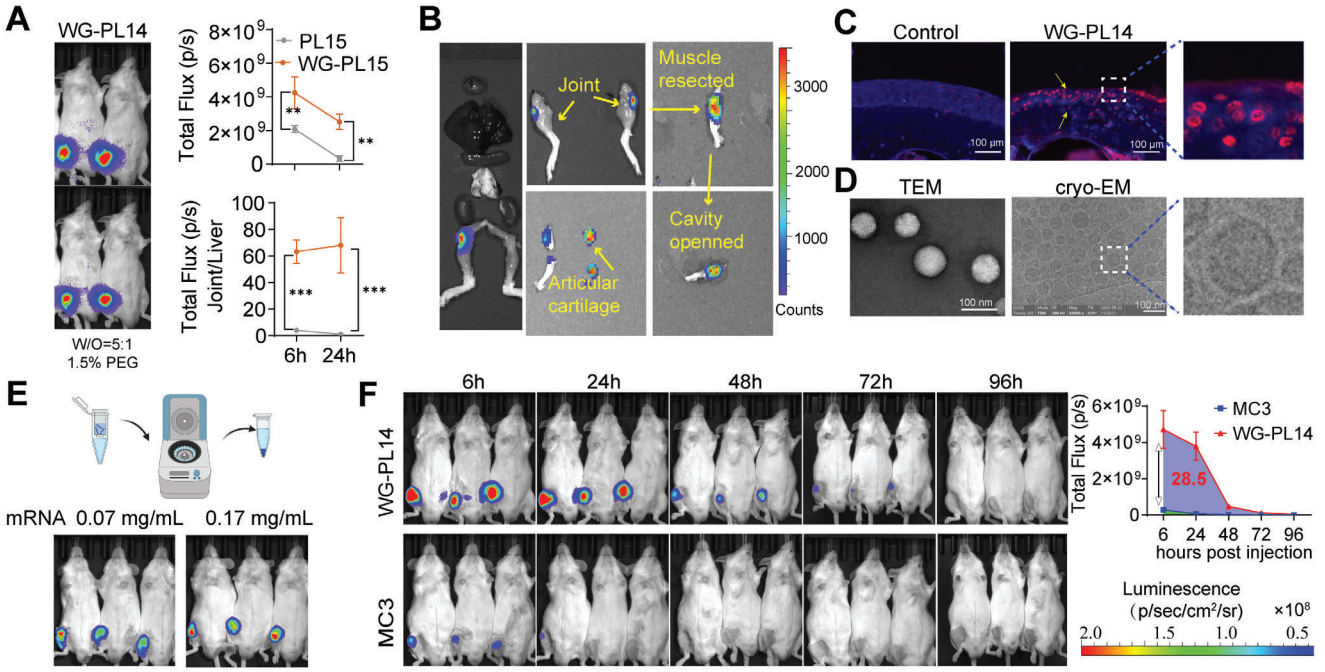

Figure 2. Comparison of the top performing WG-PL14 LNPs with MC3 LNPs for intra-articular injections. A) Representative biodistribution image of luciferase expression for original and optimized formulation LNP. B) The biodistribution image of luciferase expression in articular cartilage as measured with an IVIS imaging system 24 h after intra-articular injection of 2 μg of total mRNA. C) Immunofluorescence staining for Luc in mouse chondrocytes after intra-articular injection of LNP-Luc mRNA (2 μg mRNA). The yellow arrows indicate the luminescent zone. D) Representative TEM and STEM of LNPs. E) The biodistribution image of luciferase expression in articular cartilage after intra-articular injection of concentrated and unconcentrated LNP-Luc mRNA (2 μg mRNA). F) The comparison between WG-PL14 and MC3 in vivo expression, after injection of LNP-Luc mRNA (2 μg mRNA), then imaged in 6, 24, 48, 72, and 96 h. Data were represented as mean ± SEM. Statistical significance was calculated by *t*-test. The unit of the fluorescent scale bar is photons/sec/cm^2/sr, the F radiance scale of 1.0×10^7–2×10^8 ($^*p < 0.05$, $^{**}p < 0.01$, and $^{***}p < 0.001$).

that the inclusion of long-alkyl chain PEG decreased local mRNA expression while increasing systemic mRNA expression (Figure S2C, Supporting Information). Therefore, using C14-PEG, along with a lower percentage, allows for a balance between LNPs penetration and the gradual shedding of PEG, which ultimately facilitates uptake and expression.

Moreover, it is worth noting that in the context of the osteoarthritis model, there is a decrease in the microenvironment pH. Given that our WG-PL14 LNPs possess a surface pKa of pH 6.8, they are expected to undergo gradual ionization despite exhibiting a slight negative charge at the physiological pH (Figure S2B, Supporting Information). Collectively, the optimization of our formulation indicates that the interplay between particle size, charge, and PEG shedding plays a significant role in facilitating the efficient delivery and expression of LNPs in chondrocytes.

By combining adjustments to the PEG content and W/O ratio (the final formulation: 1.5% PEG, W/O = 1:5, N/P = 9, and 50 mM dialysis buffer), we achieved an overall net-negative charge (Figure S2A, Supporting Information) and particle sizes ranging from 100 to 200 nm (Figure S1A, Supporting Information). The final LNPs exhibited a spherical morphology under TEM and cryo-TEM (**Figure 2D**), possessed a pKa of ≈6.8 (Figure S1B, Supporting Information) and the mRNA encapsulation efficiency was 82%. In comparison to the original formulation, mRNA expression was twofold higher at 6 h and nearly tenfold higher at 24 h. The joint-to-liver ratio consistently exceeded 60-fold (Figure 2A). To confirm the specific expression of mRNA within the joint, we resected muscles and exposed the articular cartilage cavity (Figure 2B). IVIS images primarily indicated mRNA expression within the cavity, and fluorescent imaging revealed specific expression within the chondrocytes, penetrating deeper into the bone's central region (Figure 2C). In comparison to the FDA-approved lipid Din-Lin-MC3 (MC3), commonly used for mRNA delivery, our final formulation exhibited over 15-fold higher mRNA expression at 6 h post-dosing (Figure 2F). The expression remained detectable for 96 h, representing an almost 30-fold increase compared to MC3-delivered mRNA over the same period. Also, compared with the noncapsulated free mRNA, the fluorescent was nearly 10^3-fold higher in the WG-PL14-mRNA group (Figure S1C, Supporting Information). In another study, we were able to demonstrate that the fluorescence-labeled finalized formulation, when co-incubated with cartilage, exhibited enhanced localization to the cartilage (Figure S3, Supporting Information).

Considering that therapeutic RNA often requires higher dosages in lower volumes, we evaluated the impact of LNP concentration on intra-articular injection. By utilizing ultra-filtration, we concentrated the LNPs, resulting in a concentrated mRNA solution with a concentration of ≈0.17 mg mL^{-1} compared to the original 0.07 mg mL^{-1}. There is no difference between WG-PL14 and post-filtration WG-PL14 in size, PDI, and Zeta potential (Figure S4, Supporting Information). Importantly, we observed no changes in encapsulation efficiency, morphology, or mRNA expression following injection, indicating the feasibility of

© 2024 The Author(s). Advanced Healthcare Materials published by Wiley-VCH GmbH

concentrating LNPs for therapeutic applications via intra-articular injections (Figure 2E). Moreover, we evaluated the stability of the optimized WG-PL14 LNPs upon storage at 4 °C. As shown in Figure S5 (Supporting Information), WG-PL14 LNPs remained stable over a 20-day period, with no significant changes observed in terms of particle size, polydispersity index (PDI), or zeta potential (Figure S5A, Supporting Information). Additionally, the in vivo mRNA delivery efficiency of the WG-PL14 LNPs remained consistent between day 0 and day 20 (Figure S5B, Supporting Information). These results indicate that our final WG-PL14 mRNA LNP formulation, similar to the commercially available MC3 LNP formulation, maintains its physicochemical properties and bioactivity during long-term storage.

Overall, our initial formulation screening demonstrated that the final formulation, featuring slightly larger particle sizes and a net negative charge, enables specific delivery of mRNA to the joint without off-target systemic distribution. Furthermore, concentrating LNPs allows for higher dosage delivery, facilitating the achievement of locally therapeutic concentrations.

2.2. rhFGF18 mRNA Translated to Functional Protein in Rat Chondrocytes

Next, we designed a rhFGF18 mRNA sequence via optimizing the 5′UTR and 3′UTR region and performing codon-optimization on the rhFGF18 coding sequence (CDS) (Figure S6A, Supporting Information). Then we sought to determine the biological functionality of the rhFGF18 mRNA utilizing isolated primary rat chondrocytes and mouse OA model. Considering the differences between species, we made a comparison of the FGF18 sequence among humans, mice, and rats with the canonical CDS (Figure S6B, Supporting Information). We found only three different amino acids located in the signal sequence or the chain of FGF18, which means rhFGF18 possibly maintained its function in mice and rats.

To assess the transfection efficiency of rat chondrocytes, we initially transfected EGFP mRNA into the cells using Lipofectamine RNAiMAX transfection reagent. Cells were subjected to further analysis 12 h post-transfection. Confocal microscope imaging revealed intense green fluorescence compared to the control group (**Figure 3A**). Fluorescence-activated cell sorting (FACS) analysis indicated a tenfold increase in EGFP signaling in the transfected group (Figure 3B). Further statistical analysis confirmed that 92.3% of rat chondrocytes were successfully transfected with EGFP mRNA (Figure 3C). The above results demonstrated that a relatively high transfection efficiency of mRNA could be reached in rat chondrocytes via chemical transfection, which provides a suitable way to deliver rhFGF18 mRNA into rat chondrocytes.

Next, to evaluate the biological functionality of rhFGF18 mRNA, rat chondrocytes were transfected with rhFGF18 mRNA using the method mentioned above. Immunostaining on FGF18 reveals widespread expression of rhFGF18 in the cytoplasm (Figure 3D), with significantly different fluorescent intensities between control and transfected groups (Figure 3E). Expression of rhFGF18 in rat chondrocytes was also validated via Western Blot (Figure 3F). Moreover, rhFGF18 could be detected in the supernatant (Figure 3G). The concentration of rhFGF18 protein in the supernatant continuously increased from 12 h post-transfection to 96 h (Figure S6D, Supporting Information). These results suggested that the in vitro transcribed rhFGF18 mRNA could be translated into rhFGF18 protein and correctly secreted by rat chondrocytes.

Previous studies indicated the positive impact of rhFGF18 protein on chondrocyte proliferation.[25] To investigate whether rhFGF18 in the supernatant has similar biological effects, we transfected rat chondrocytes with rhFGF18 mRNA and collected the supernatant as a conditional medium (CM). Supernatant from cells transfected with EGFP mRNA served as the control. Subsequently, rhFGF18 mRNA CM and control CM were used to culture additional batches of chondrocytes to test whether rhFGF18 accelerated the proliferation of the cells. Indeed, discrepancies in cell numbers were significant from day 2 (Figure 3H), with the rhFGF18 mRNA CM-cultured cells showing a 2.5-fold increase over the control group by day 3 (Figure 3I). EdU (5-ethynyl-2′-deoxyuridine) assay was conducted, and after 3 h of EdU labeling, cells cultured with rhFGF18 mRNA CM exhibited ≈35% positive rate, whereas the control group showed only ≈21% positive rate (Figure 3J; Figure S2C, Supporting Information). This suggests enhanced cell proliferation under rhFGF18 stimulation. We also performed FACS analysis on Ki-67, a typical proliferation marker. A slight shift appears between rhFGF18 and the control group, indicating the upregulation of Ki-67 expression (Figure S6E, Supporting Information). CCK-8 assay indicated improved cell survival in rhFGF18 mRNA CM (Figure 3I). Overall, our findings demonstrate that the secreted rhFGF18 protein promotes chondrocyte proliferation, implying the potential therapeutic effects of rhFGF18 mRNA in OA.

2.3. Characterization on the Transcriptome of Human Chondrocyte After Treating with rhFGF18 mRNA CM

To further elucidate potential distinctions among chondrocytes treated with different CM, we isolated human primary chondrocytes from intact areas (healthy group) or damaged areas (OA group) in femoral condyles of total knee arthroplasty patients and conducted RNA sequencing (RNA-seq) analysis after treated with control CM and rhFGF18 mRNA CM for 24 h. Principal components analysis and pairwise correlation analysis revealed substantial differences after rhFGF18 mRNA CM treatment (**Figure 4A,B**). To gain a deeper understanding of the transcriptional variances, we found the co-upregulated genes after rhFGF18 mRNA CM stimulation in healthy and OA groups (Figure 4C; Figure S7A, Supporting Information). The co-upregulated genes included BMP2 and FGF2, the canonical growth factors belonging to BMP and FGF signaling, also AGRN and HAS2, the proteins related to ECM synthesis. We found the chromatin remodeling factor, HMGA2, which was previously reported in Lin28a-induced chondrocyte reprogramming and cartilage anabolism, was also upregulated after rhFGF18 CM treatment.[26] These results indicated that rhFGF18 protein translated from rhFGF18 mRNA could promote chondrocyte proliferation and ECM synthesis. We also conducted gene ontology (GO) enrichment analysis between the different treated groups and “response to hypoxia”, “heme binding” and “growth factor activity” were on top ranks (Figure 4D). To further elucidate the downstream targets of rhFGF18, we performed gene set

© 2024 The Author(s). Advanced Healthcare Materials published by Wiley-VCH GmbH

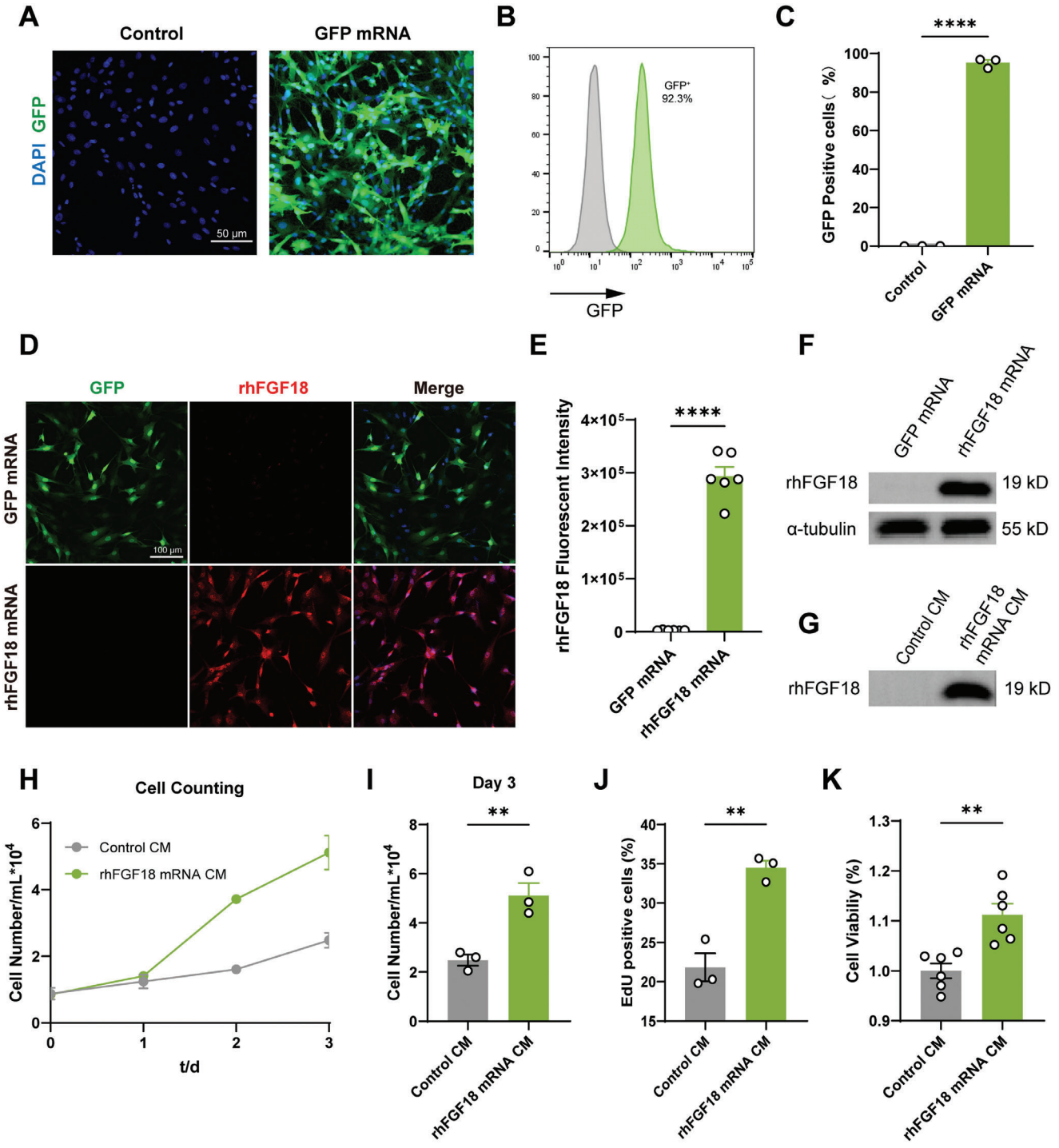

Figure 3. In vitro transfection and characterization of GFP and rhFGF18 mRNA. A) Representative images of rat primary chondrocytes 24 h post-GFP mRNA transfection. B) Flow cytometry analysis of rat primary chondrocytes 24 h post-GFP mRNA transfection. C) Statistical analysis of GFP positive cells between control and GFP mRNA group. D) Representative images of immunofluorescence of rat primary chondrocytes 24 h post-rhFGF18 mRNA transfection or GFP mRNA transfection. E) Quantification of the immunofluorescence images. Western blot analysis of F) total protein and G) supernatant of rat primary chondrocytes 24 h post-rhFGF18 mRNA transfection or GFP mRNA transfection. Rat primary chondrocytes cultured with control CM and rhFGF18 mRNA CM and perform H) cell counting on day 1,2,3, I) statistical analysis of cell numbers on day 3, J) Quantification of flow cytometry analysis on EdU positive cells, K) CCK8 assays to assess cell viability. Data are shown as the mean ± SEM. Student's t-test was used for C), E), I), J), and K). $^{*}p < 0.05$, $^{**}p < 0.01$, and $^{***}p < 0.001$.

© 2024 The Author(s). Advanced Healthcare Materials published by Wiley-VCH GmbH

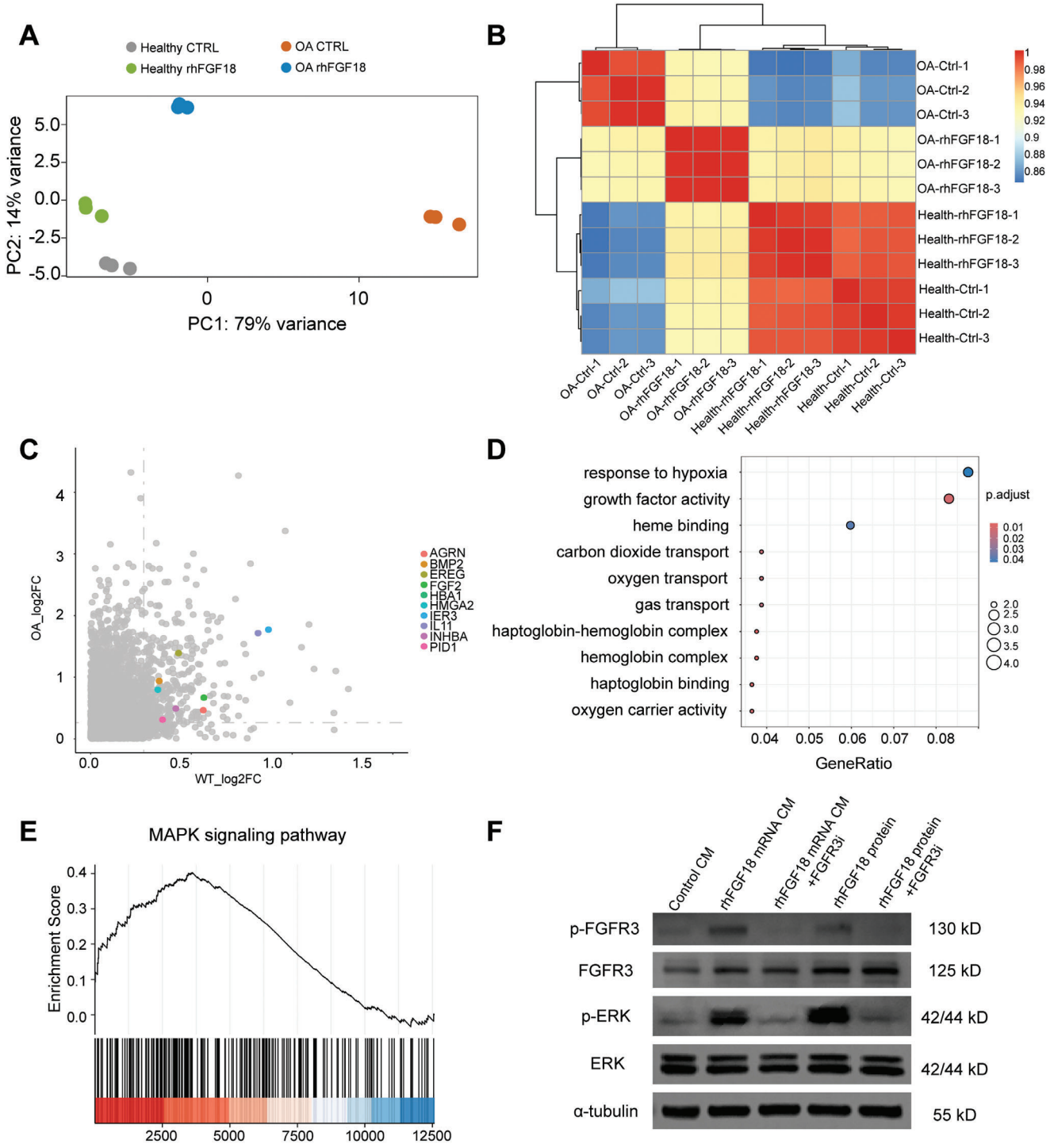

Figure 4. Transcriptome analysis of human primary chondrocytes after rhFGF18 mRNA CM stimulation. A) Principal component analysis (PCA). B) Pairwise correlation based on Pearson coefficients between all samples. C) Genes co-upregulated in chondrocytes from healthy or osteoarthritis areas after stimulation of rhFGF18 mRNA CM. D) Gene ontology analysis between chondrocytes cultured with rhFGF18 mRNA CM and control CM. E) Gene set enrichment analysis (GSEA) reveals MAPK signaling pathway-related genes enriched in chondrocytes cultured with rhFGF18 mRNA CM. F) Western blot analysis on phosphorylation of key components of MAPK signaling pathway.

© 2024 The Author(s). Advanced Healthcare Materials published by Wiley-VCH GmbH

enrichment analysis (GSEA) and found that the rhFGF18 mRNA CM treated group enriched for MAPK signaling pathway-related genes, which suggested rhFGF18 potentially activated MAPK signaling to promote proliferation. We used stringDB to the ligand of FGF18, and FGFR3 was found (Figure S7B, Supporting Information). This prediction was consistent with the previous report that FGF18 is a high-affinity ligand of FGFR3.[6] Indeed, phosphorylation of FGFR3 and ERK1/2 was detected after rhFGF18 mRNA CM or rhFGF18 protein treatment, and the related bands disappeared after derazantinib, a FGFR3 kinase inhibitor (FGFR3i) treatment (Figure 4F; Figure S3F, Supporting Information). Notably, the concentration of rhFGF18 in CM was ≈20 ng mL^{-1}, but still had a similar effect as 2 µg mL^{-1} rhFGF18 protein treatment in western blot analysis, indicating the chondrocyte-derived endogenous rhFGF18 is more effective in activating key components of MAPK signaling (Figure S7G,H, Supporting Information). We also found the enrichment of proliferation-related, ECM-related, and tyrosine phosphorylation-related gene sets via GSEA (Figure S7C–E, Supporting Information).

2.4. Intra-Articular Injection of rhFGF18 mRNA Ameliorated OA Progress in Mouse

Next, our objective was to explore the potential of intra-articular LNP-rhFGF18 mRNA injection in alleviating the progression of OA following anterior cruciate ligament transection (ACLT) in ICR mice. Saline, LNP-Luc mRNA, LNP-rhFGF18 mRNA, or rhFGF18 protein was administered at 2, 3, and 4 weeks to the knee joint (**Figure** 5A). In accordance with a previous study on intra-articular injection in mice, we administered 2 µg of rhFGF18 mRNA or Luc mRNA per leg for the in vivo investigation.[27] Considering that OA-induced pain constitutes a primary focus in the treatment of OA, we evaluated pain response using the hotplate test. The results demonstrated that the intra-articular injection of LNP-rhFGF18 mRNA in ACLT mice significantly prolonged the response time of mice at 8 weeks post-surgery (Figure 5B). Given the pivotal role of the bone–cartilage unit in joint homeostasis and OA development, targeting abnormal subchondral bone remodeling becomes crucial for pain relief and OA treatment.[28] Micro-CT (µCT) analysis was employed to assess subchondral bone tissue changes with the aforementioned treatments in ACLT mice. The µCT images of the knee joints revealed that LNP-rhFGF18 mRNA or rhFGF18 protein treatment significantly decreased osteophyte formation compared to saline treatment (Figure 5C). Additionally, an uneven distribution of bone mass and partial loss of bone volume were observed in saline-treated ACLT mice relative to LNP-rhFGF18 mRNA or rhFGF18 protein-treated groups (Figure 5C), indicating disordered subchondral bone formation during post-traumatic OA development. Quantitative analysis of the tibial subchondral trabecular bone showed that the trabecular pattern factor (Tb. Pf) was significantly higher in the saline-treated group than in sham or LNP-rhFGF18 mRNA or rhFGF18 protein-treated mice (Figure 5D) after 8 weeks, indicating improved disruption of the connectivity and microarchitecture of trabecular bone.[29] Meanwhile, we observed a significant improvement in trabecular bone volume per total volume (BV/TV) and trabecular thickness (Tb.Th) after LNP-rhFGF18 mRNA or rhFGF18 protein administration (Figure 5E,F) in ACLT animals. Similar to the sham mice, the bone mineral density (BMD) of the tibia subchondral bone medial compartment was greater in the ACLT mice with LNP-rhFGF18 mRNA or rhFGF18 protein treatment when compared to that in the control groups at 8 weeks post-operatively (Figure 5G). We also conducted the above-described experiments at 4 weeks post-operatively and the results were consistent (Figure S8A–G, Supporting Information). In conclusion, intra-articular injection of LNP-rhFGF18 mRNA demonstrated positive effects in ameliorating the OA-related symptoms.

To further evaluate the therapeutic efficacy of LNP-rhFGF18 mRNA at the histological level, we conducted various routine stainings on cartilage tissue sections. Safranin O-fast green staining revealed a reduction in proteoglycan loss and preservation of cartilage structure in ACLT mice treated with LNP-rhFGF18 mRNA compared to control groups (**Figure** 6A). To ascertain whether rhFGF18 mRNA promotes cartilage proliferation in vivo, H&E staining was performed, and cell numbers were quantified based on nuclear staining. The results demonstrated a significant increase in the number of chondrocytes following LNP-rhFGF18 mRNA treatment (Figure 6B). IHC staining for Collagen II, Aggrecan, Mmp13, Collagen I, and IL-1β (Figure 6C) was conducted to assess the impact of intra-articular injection of rhFGF18 mRNA on ECM metabolism in cartilage. As anticipated, the expressions of both Collagen II and Aggrecan exhibited significant enhancement after LNP-rhFGF18 mRNA treatment (Figure 6E,F). Meanwhile, Mmp13, a protease responsible for breaking down collagen,[30] decreased in cartilage tissue following LNP-rhFGF18 mRNA treatment compared to the control groups, suggesting that LNP-rhFGF18 mRNA inhibits ECM catabolism (Figure 6G). Additionally, the expression of Collagen I, a marker of fibrous cartilage, and IL-1β, a proinflammatory cytokine decreased after treatment, confirming the anti-inflammatory role of rhFGF18 mRNA (Figure 6H,I). The conclusion was further confirmed by performing the above analyses in 4-week post-treatment joint samples (Figure S9A,G, Supporting Information).

Furthermore, to confirm the nontoxic nature of LNP-rhFGF18 mRNA injection in mice, we conducted anatomical examinations of the heart, liver, kidney, lung, and spleen through hematoxylin and eosin (H&E) staining and no significant differences were observed (Figure S10A, Supporting Information). Additionally, we conducted a complete blood count and comprehensive metabolic panel across different experimental groups. The results exhibited a consistent profile between the saline-administered group and the groups treated with LNP-mRNA, underscoring the nontoxic attributes of LNP-rhFGF18 mRNA as an OA treatment (Figure S10B, Supporting Information).

3. Discussion

Our study advances an efficient approach to articular cartilage tissue regeneration and osteoarthritis therapy by introducing of LNP-rhFGF18 mRNA complex via intra-articular injection to enhance therapeutic benefits. To make the LNP retained in the joint cavity, we made modifications to the original formulation to overcome issues with LNP leakage into the systemic circulation and mRNA expression in the liver. Then, we design an optimized

© 2024 The Author(s). Advanced Healthcare Materials published by Wiley-VCH GmbH

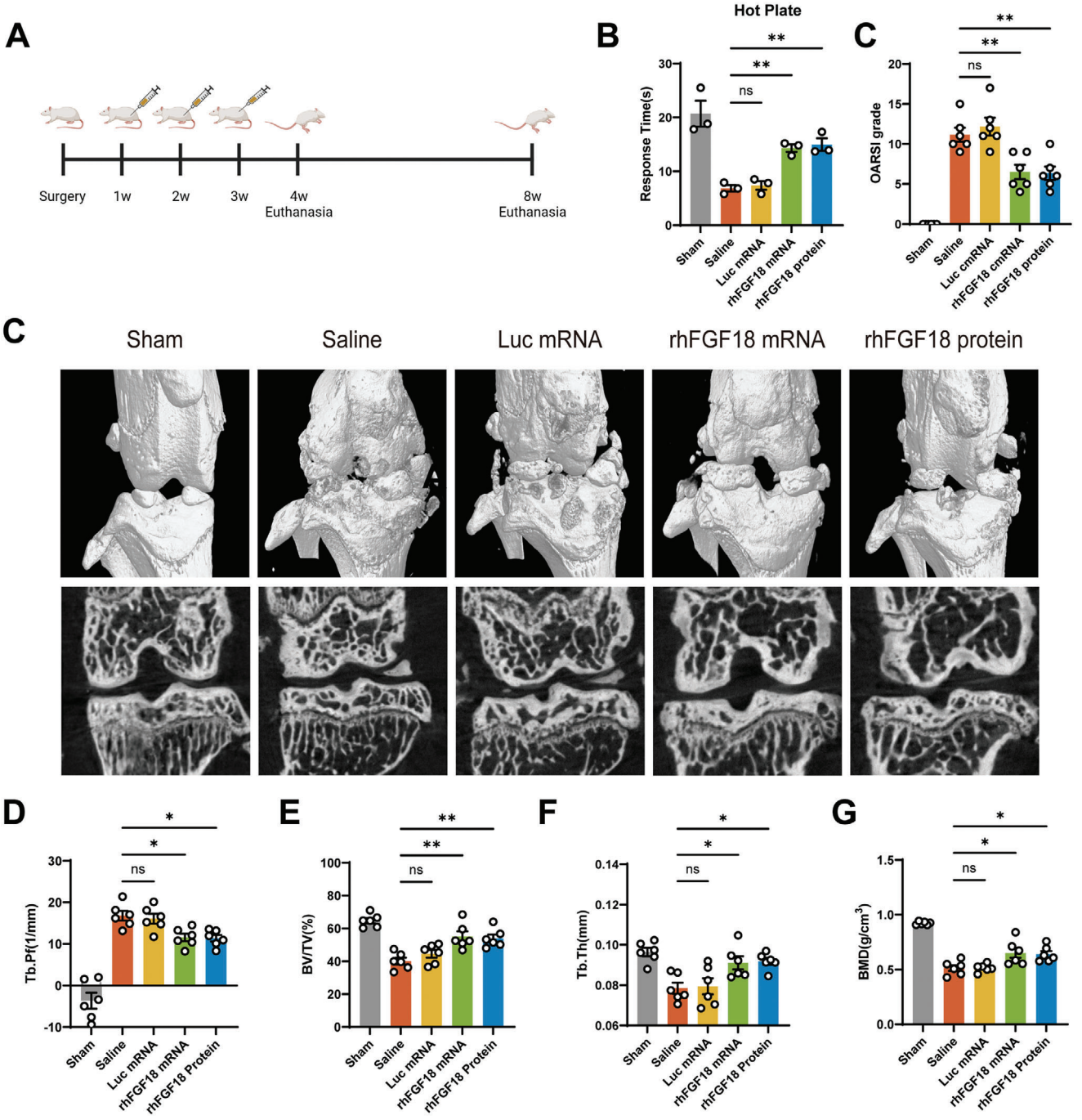

Figure 5. WG-PL14-rhFGF18 mRNA prevents against the progression of post-traumatic OA in vivo. A) Schematic diagram of the timeline of intra-articular injection of LNP-rhFGF18 mRNA and subsequent analysis. B) Pain response time after placing the mice onto a 55 °C hot plate meter at 8 weeks post-surgery. C) Representative micro-CT (μCT) images of the joints from mice treated with saline, LNP-luc mRNA, LNP-rhFGF18 mRNA, or rhFGF18 protein at 8 weeks after sham or ACLT surgery. $n = 6$ for each group. Quantitative μCT analysis of tibia subchondral bone parameters including D) trabecular bone pattern factor (Tb.Pf), E) trabecular bone volume per tissue volume (BV/TV), and F) trabecular thickness (Tb.Th) and G) bone mineral density (BMD) in each group at 8 weeks postoperatively. $n = 6$ for each group. Data are shown as the mean ± SEM. One-way ANOVA was used for D), E), F), and G). $^{*}p < 0.05$, $^{**}p < 0.01$, and $^{***}p < 0.001$.

© 2024 The Author(s). Advanced Healthcare Materials published by Wiley-VCH GmbH

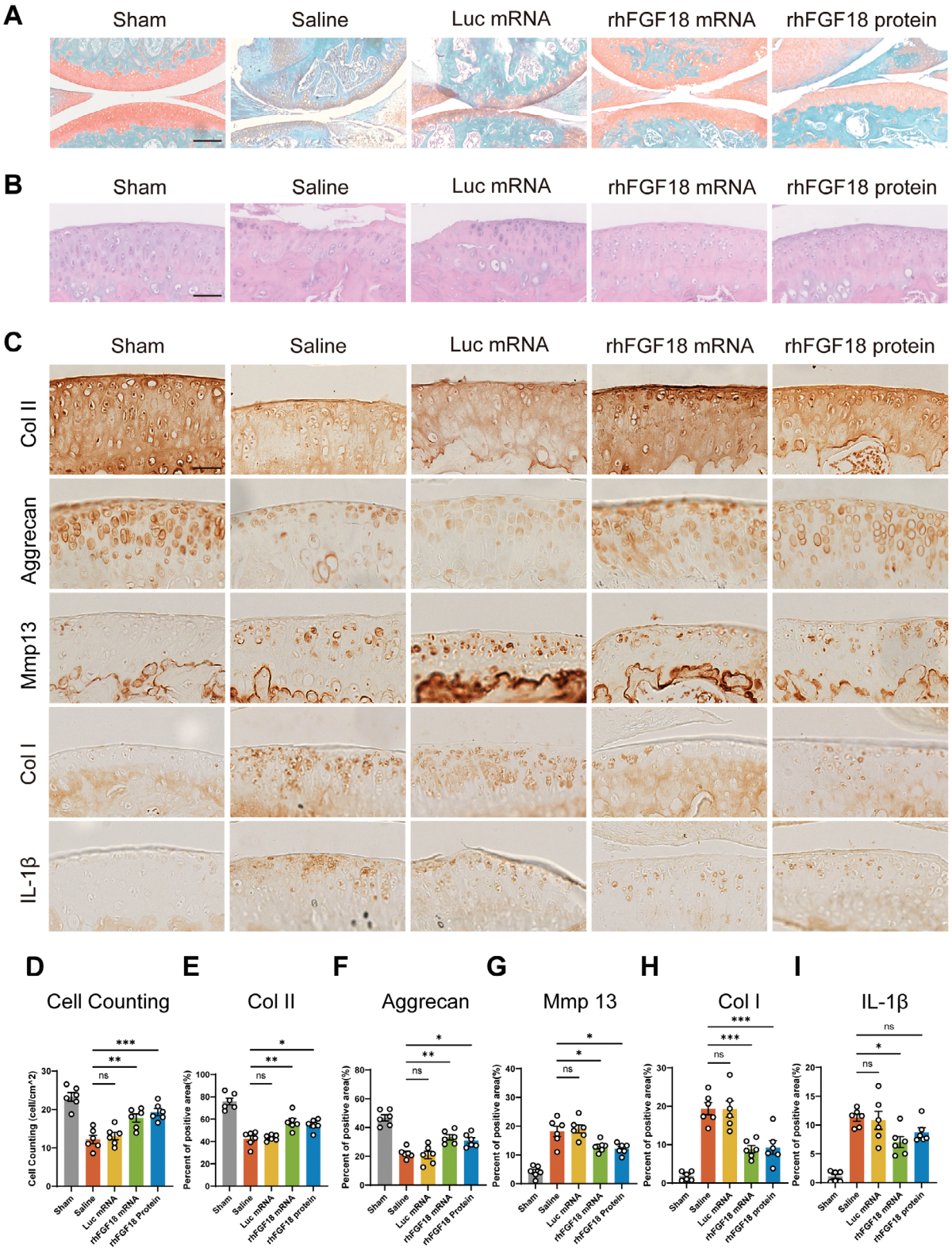

Figure 6. LNP-rhFGF18 mRNA intra-articular injection enhanced chondrocyte proliferation and matrix anabolism. A) Safranin O-fast green staining, B) H&E staining, and C) IHC staining for Collagen II, Aggrecan, Mmp13, Collagen I, and IL-1β of mouse knees at 8 weeks post intra-articular injection of LNP-rhFGF18 mRNA. Quantification of D) cell numbers in H&E staining and positive area in IHC staining of E) Collagen II, F) Aggrecan, G) Mmp13, H) Collagen I and I) IL-1β. $n = 6$ in each group. "n" represents the number of mice. Data are shown as the mean ± SEM. Scale bars, 200 µm for A) and 50 µm for B) and C). One-way ANOVA was used for D), E), F), G), H), and I). $^{*}p < 0.05$, $^{**}p < 0.01$, and $^{***}p < 0.001$.

© 2024 The Author(s). Advanced Healthcare Materials published by Wiley-VCH GmbH

rhFGF18 mRNA sequence and fully characterize the biological functionality and the potential in OA treatment of the rhFGF18 mRNA via in vitro and in vivo experiments. The results demonstrate that the chemically nucleoside-modified mRNA therapy is an effective, safe, and affordable approach for potential clinical translation.

OA is a multifactorial, chronic, degenerative joint disease characterized by cartilage loss, subchondral bone remodeling, osteophyte formation, and synovial inflammation. These processes contribute to joint pain and functional impairment, posing a significant and escalating health burden, carrying noteworthy implications for the affected individuals, healthcare systems, and broader socioeconomic costs.[31,32] However, OA treatment options remain limited, and there is a lack of drugs that can reverse the progress. The current pharmaceutical treatments recommended by international guidelines for OA are primarily symptomatic, characterized by relatively small effect sizes, and present uncertainties regarding their long-term efficacy and safety.[33,34] Progressive cartilage breakdown is a major therapeutic target for putative disease-modifying OA drugs (DMOADs). Promoting cartilage repair represents a potential approach to counter cartilage loss in OA. A significant advancement in anabolic treatments involves sprifermin. Preclinical studies have identified FGF18 as a crucial anabolic factor, influencing chondrogenesis, chondrocyte proliferation, and cartilage repair in both healthy and damaged cartilage through the activation of FGFR3.[8,9,35] Supporting these findings, sprifermin demonstrated the stimulation of matrix production by porcine chondrocytes when administered intermittently.[25] In bovine explants, sprifermin induced ECM turnover, elevating the production of type II collagen and aggrecan, particularly in the absence of proinflammatory stimuli.[36] However, the nature of the articular cartilage niche is resistant to the penetration of macromolecules.[37] Also, direct delivery of protein may not be suitable for chronic dosing due to a relatively large amount of required dose.[38] These highlighted a crucial need to develop a new way for rhFGF18 delivery.

RNA-based therapies engineered through synthetic chemistry show great promise for future treatments of OA. These therapies offer enduring and effective mechanisms of action, precisely targeting the fundamental drivers of pathology. In comparison to protein drugs, mRNA therapeutics have a distinct advantage in their ability to synthesize high levels of intracellular proteins.[38] Optimizing the 5′ cap structure and the sequence of 5′ UTR, 3′ UTR, poly-A tail, and CDS can enhance the stability and translation efficiency of mRNA. The delivery of mRNA acts as an intracrine approach, leading to the translation of proteins with multiple posttranslational modifications (PTMs) associated with the secreting cells. It is important to note that these PTMs may result in biological functionality differences between the mRNA-derived protein and in vitro purified protein. Indeed, we observed that the chondrocyte-derived endogenous rhFGF18 is more effective, reflecting that 20 ng mL^{-1} endogenous protein can have similar effects as 2 µg mL^{-1} rhFGF18 protein does. This suggests that, at least in rhFGF18 therapy, mRNA offers advantages in low dosage, leading to a more cost-effective treatment and compatibility with chronic dosing.

As articular cartilage is avascular, systemic drug delivery is ineffective. Direct intra-articular injections are preferred, particularly since OA predominantly affects the local joint environment.[39,40] Injected drugs, however, face the challenge of brief joint residence time as they quickly exit the synovium vasculature and lymphatics.[40,41] Moreover, these drugs encounter difficulty reaching their target sites within the deep zones of affected joint tissues, such as cartilage, due to the dense meshwork of collagen and aggrecan proteoglycans. These components contain highly negatively charged glycosaminoglycan chains that impede the penetration of most macromolecules.[37,42] Therefore, it is crucial to develop materials with the ability to penetrate cartilage. Following intra-articular administration, these materials should facilitate the swift uptake of drugs throughout the entire thickness of the cartilage, ensuring the attainment of therapeutic levels before clearance. Additionally, they should have the capacity to bind within the cartilage, augmenting joint residence time. LNPs stand at the forefront mRNA delivery system, enhancing RNA stability and in vivo delivery efficiency. LNPs possess the following key advantages: 1) mRNA is encapsulated within the core of LNPs, effectively shielding it from degradation by RNase enzymes; 2) LNPs can mimic the spontaneous endocytosis of low-density lipoproteins, leading to high cellular uptake efficiency; 3) In the neutral environment of the body, LNPs exhibit an overall neutral charge, resulting in low biological toxicity.[21,43,44] Meanwhile, topical administration routes for mRNA therapeutics have been investigated to achieve local therapeutic effects. For instance, local injection of lipid nanoparticle-mRNA formulations allows the supplementation of therapeutic proteins in specific tissues like the heart,[45] eyes,[46] and brain.[47] However, studies in delivering LNP-mRNA complex toward the articular cavity are still lacking. In this study, we optimized the LNP formulation by combining adjustments to the PEG content and W/O ratio and achieved an overall net-negative charge to facilitate the delivery of mRNA into the cartilage tissue. The final LNPs have high encapsulation efficiency and exhibit significantly strong bioluminescence at the joint cavity when delivering firefly luciferase mRNA. The established new LNP formulation is a good resource for further study utilizing mRNA to treat OA.

A recent research paper introduced a CRISPR-based system to activate the endogenous rat *Fgf18* gene for OA therapy, highlighting the potential of CRISPR-based FGF18 treatment in OA treatment.[48] This method employed hybrid exosomes incorporating the chondrocyte-affinity peptide (CAP) for delivering dCas9, MS2-p65-HSF1 protein, and sgRNA plasmid, achieving long-term expression of Fgf18 from endogenous *Fgf18* locus. Additionally, another study developed an AAV2-FGF18 strategy aimed at achieving prolonged FGF18 production with a single injection.[49] While these gene therapies offer potential solutions for the long-term mitigation of OA symptoms with fewer administration times, LNP-mRNA-based therapy presents the advantages of enhanced safety and a shorter timeline for clinical translation. Overall, the development of novel FGF18 delivery and expression methods, encompassing both CRISPR and AAV-based and mRNA-based therapies, brings significant advances in OA treatment.

The present study is not without limitations. While we assessed the effectiveness of LNP-rhFGF18 mRNA treatment in a post-traumatic OA mouse model, our experiments do not cover the entire spectrum of OA disease. Further investigation is required to explore the potency of this treatment in OA animals

© 2024 The Author(s). Advanced Healthcare Materials published by Wiley-VCH GmbH

driven by other mechanisms, such as natural aging or obesity. Given that the clinical application of FGF18 protein has primarily been on patients with severe OA symptoms, it is essential to comprehensively evaluate and compare the therapeutic effects of protein-based, CRISPR-based, and mRNA-based FGF18 therapies in a mouse OA model with similarly pronounced symptoms as well. Also, this study primarily focused on the therapeutic efficacy of a single delivery of rhFGF18 mRNA. However, it is essential to consider combining rhFGF18 mRNA treatment with anti-inflammatory treatment in OA to further ameliorate the disease progress. Co-delivery of multiple anti-inflammatory cytokines like IL-6 mRNA and IL-10 mRNA could potentially yield better outcomes. Future research should address this aspect to comprehensively evaluate the therapeutic potential of mRNA treatments for OA. Moreover, it is essential to acknowledge the need for further evaluation in large-animal models. This step is crucial to establish the potential benefits of rhFGF18 mRNA therapy before its translational application in human patients since the existence of species variation. Expanding the scope of our investigations to include larger animal models will provide valuable insights into the safety and efficacy of the treatment, contributing to its overall translational relevance.

4. Conclusion

Overall, this study shows that LNP-rhFGF18 mRNA treatment in mouse OA model has a clear therapeutic benefit leading to ameliorate of OA progress, consistent with previous reports.[25,50,51] The optimized LNP formulation has a nearly 30-fold increase in mRNA expression as well as better articular cavity enrichment compared to commercial lipids MC3. And the presented experiments demonstrate, for the first time, that rhFGF18 mRNA can be translated into a functional therapeutic protein in rat and human primary chondrocytes, and shows therapeutic effects in mice. Most importantly, rhFGF18 mRNA can work with a relatively low dosage, which shows a proof of concept for the advantage of mRNA therapy in treating OA.

5. Experimental Section

LNP Materials: The ionizable lipids DLin-MC3-DMA (MC3) were purchased from Avanti Polar Lipids, Inc. Helper lipids containing 1,2-Dioleoyl-sn-glycero-3-phosphoethanolamine (DOPE), cholesterol, and 1,2-dimyristoyl-rac-glycero-3-methoxypolyethylene glycol-2000 (DMG-PEG2000) were bought from A.V.T. Pharmaceutical Tech Co., Ltd.

LNP Formulation and Characterization: LNP mRNA systems were formulated in Figure S1 (Supporting Information). All formulations were formulated by first dissolving lipids (ionizable lipid, DOPE/DSPC, cholesterol, DMG-PEG2000) into ethanol, and then the oil phase was rapidly mixed with an aqueous solution of mRNA at pH 4 citrate buffer using a microfluidic chip device at a 1:3 ethanol/water ratio. The resulting mixture was dialyzed overnight using pH 7.4 PBS. The LNP is concentrated in 10 kDa Amicon ultracentrifugation units (EMD Millipore Corporation, Billerica, MA, USA). The size, PDI, and zeta potential of nanoparticles were measured by NanoZS Zetasizer (Malvern, Westborough, MA, USA). The mRNA encapsulation efficiency (EE%) was calculated as 1-(sample without Triton X-100/sample with Triton X-100) via a RiboGreen assay. The morphology of LNP was characterized by transmission electron microscopy (TEM) and cryo-electron microscopy (cryo-EM). For cryo-EM, the prepared LNP was dialyzed in 20 mM Tris (pH 7.4) containing 8% sucrose 4 °C overnight and then concentrated to 0.5 mg mL^{-1} total RNA by ultrafiltration. Cryo-EM image was acquired using Themis 300 (Thermo Fisher Scientific).

In Situ Determination of pKa Using TNS: The apparent pKa of each cationic lipid was determined using a fluorescent probe 2-(p-toluidine)-6-naphthalene sulfonic acid (TNS) and preformed LNPs composed of cationic lipid/DOPE/cholesterol/PEG-lipid (35:16:46.5:2.5 mol%) in PBS at a concentration of ≈6 mM total lipid. In brief, TNS was prepared as a 100 μM stock solution in distilled water. LNPs were diluted to 100 μM of total lipids in 90 μL of buffered solutions (triplicates) containing 10 mM HEPES, 10 mM 4-morpholineethanesulfonic acid, 10 mM ammonium acetate, 130 mM NaCl, where the pH ranged from 2.71 to 11.5. Ten microliters of stock TNS were added to the LNP solutions and mixed well in a black 96-well plate. Fluorescence intensity was monitored in a Tecan Pro200 plate reader using excitation and emission wavelengths of 321 and 445 nm. With the resulting fluorescence values, a sigmoidal plot of fluorescence versus buffer pH was created. The log of the inflection point of this curve was the apparent pKa of the LNP formulation.

mRNA Synthesis and Formulation: Briefly, chemically modified mRNA encoding rhFGF18, firefly luciferase, and Cre recombinase was in vitro transcribed (IVT) by T7 RNA polymerase (Vazyme) from a linearized DNA template, which incorporates the 5′ and 3′ untranslated regions (UTRs) and a poly-A tail. mRNA sequence is optimized by mRNAid to improve stability and immunogenicity.[52] Then the sequences were cloned into an mRNA-expression vector digested with *NcoI* and *BpmI*, which contains a T7 RNA polymerase promoter, an unstructured synthetic 5′UTR, a multiple cloning site, and a 3′UTR. IVT templates were digested by BspQI and then transcribed by T7 RNA polymerase at 37 °C for 4 h. The generated RNA was further purified by magnetic beads (Vazyme).

Cell Isolation and Culture: Human primary normal chondrocytes or OA chondrocytes were isolated from intact area or damaged areas in femoral condyles of total knee arthroplasty patients, respectively, with the approval of the Human Ethics Committee of Peking University Third Hospital (ethical approval No.: 2013003). The patient's informed consent was obtained. The primary chondrocytes from rats and humans were cultured in minimum essential medium alpha (MEM-α; HyClone) supplemented with 10% fetal bovine serum (FBS; Gibco, USA) and 1% penicillin/streptomycin (P/S; 100 units mL^{-1} penicillin and 100 μg mL^{-1} streptomycin, HyClone). HEK293T cells were cultured in high-glucose Dulbecco's modified Eagle's medium (HG-DMEM; Procell, China). Cells were routinely passaged using TrypLE Express (Gibco). All cells were cultured in a humidified incubator at 37 °C and 5% CO_2.

mRNA Transfection: Transfection of mRNA was performed when cell confluency reached ≈60%. Lipofectamine RNAiMAX (Thermo) transfection reagents and mRNA were respectively diluted in Opti-MEM media (Invitrogen), then pooled together and incubated at room temperature (RT) for 10 min to generate the transfection mixture. 9 μL of Lipofectamine RNAiMAX transfection reagent were applied per 2 μg of mRNA. Rat chondrocytes were incubated with the transfection mixture for 6 h. Then the medium was changed to MEM-α with 10% FBS.

Immunocytochemistry: Cells were washed with PBS, fixed with 4% paraformaldehyde (PFA) for 15 min at RT, and permeabilized with 0.1% Triton-X 100 for 10 min. Cells were blocked in blocking buffer (2% BSA) for 30 min and incubated with primary antibodies diluted in blocking buffer (rhFGF18, Proteintech, 11495-1-AP, 1:50) for 30 min at RT. Cells were then washed with PBS three times and incubated with secondary antibodies diluted in a blocking buffer at 1:500 for 15 min at RT. After three times washing with PBS, cells were counterstained with 4′,6-diamidino-2-phenylindole (DAPI; 0.5 μg mL^{-1}) for 10 min. Images were captured using LSM880 (Carl Zeiss) with a 20× objective lens. Quantification of the fluorescent intensity is based on ImageJ software. Briefly, the intensity of the single cell is calculated and the background intensity is excluded. Six cells are calculated for each group.

Western Blot Analysis: Cells were lysed with RIPA Lysis Buffer (Beyotime) in the presence of a protease inhibitor and phosphatase inhibitor (Beyotime). The concentration of protein was quantified by BCA assay (Beyotime). Protein was boiled and separated on 10% SDS–polyacrylamide

© 2024 The Author(s). Advanced Healthcare Materials published by Wiley-VCH GmbH

electrophoresis gels. Then protein was transferred onto a polyvinylidene difluoride membrane. The membrane was blocked in 5% BSA at RT for 1 h and subsequently incubated with primary antibodies (rhFGF18, Proteintech, 11495-1-AP, 1:10 000; p-FGFR3, Abcam, ab-155960, 1:10 000; FGFR3, Proteintech, 66954-1-1 g, 1:2000; p-ERK1/2, Cell Signaling Technology, 4370T, 1:2000; ERK1/2, Cell Signaling Technology, 4695S, 1:2000; α-tubulin, Abclonal, AC012, 1:1000) at 4 °C overnight. The membrane was washed in Tris-buffered saline with 0.1% Tween 20 (TBST) and incubated with horseradish peroxidase (HRP)-conjugated secondary antibodies (goat anti-mouse, Thermo, C31430100, 1:10 000; goat anti-rabbit, Thermo, C31460100, 1:5000) at RT for 1 h. After being washed by TBST, the membrane was then subjected to western blot detection reagents (Beyotime) to generate a chemiluminescent signal based on the manufacturer's protocol.

Flow Cytometry: Cells were dissociated into single-cell suspensions using TrypLE and washed with PBS supplemented with 1% bovine serum albumin and 0.2 mM EDTA. In indicated experiments, cells were stained with flow cytometry antibodies and analyzed using a Guava easyCyte 6HT/2 L flow cytometer (Millipore Corporation, Billerica, MA) and FlowJo software (Tree Star Inc., Ashland, OR).

ELISA Assay: rhFGF18 in the supernatants was quantified by a human FGF18 ELISA kit (Novus, NBP3-06766) according to the manufacturer's protocol.

Animal: Experiments were approved by the Ethics Committee of Peking University (LA2022327). All experimental procedures were ethically approved and performed under the guidelines of the Care and Use of Laboratory Animals. For in vivo luciferase expression assays. The 8-week-old female ICR mice were injected with D-Luciferin potassium salt ($\approx$150 mg kg^{-1} at certain time points after injection of the Fluc mRNA LNPs, then imaged by IVIS imaging system (Perkin Elmer), Luminescence was quantified using the Living Image software (PerkinElmer). For induction of the OA model and further treatment. 8-week-old ICR mice (purchased from Peking University Health Science Center Department of Laboratory Animal Science) were subjected to anterior cruciate ligament transection (ACLT) or sham surgery. Briefly, under general anesthesia, the anterior cruciate ligament of the bilateral knee was transected. For the sham surgery group, the same procedures were performed with no ligament transection. After a week post-ACLT, the ICR mice were given an intra-articular injection (20 µL per mouse) of vehicle (saline) or mRNA (2 µg per knee joint) or rhFGF18 protein (2 µg per knee joint) once a week for three weeks. Animals were euthanized 4 weeks or 8 weeks after sham or ACLT operation.

Hot Plate Test: The pain response in the joints of mice in different experimental groups was evaluated by hot plate test. Briefly, the animals were placed on a hot plate meter (Ugo Basile SRL, Italy) at 55 °C, and the time from the point when both hind limbs touched the hot plate until the appearance of hind limb responses, such as shaking, jumping, or licking, was measured. Each animal was tested three times at 15-min intervals, and the average of the three response times was considered as the final pain threshold of the mouse. The observers were blinded to the experimental treatments.

Micro-Computed Tomography (µCT): Intact knee joints were fixed in 10% neutral buffered formalin for 48 h, then immersed in 70% alcohol for µCT scanning. The scanning started from the subchondral bone with a 6 µm resolution for 40 slices. µCT analysis was applied for the detection of osteophyte development and subchondral bone remodeling using a SKYSCAN 1276 (Bruker).

Histology, Immunohistochemistry, and Immunofluorescence: The excised whole knee joints of mice were fixed in 4% neutral-buffered PFA for 48 h. The specimens were then decalcified for 6 h in a decalcification solution (ZLI-9307; ZSGB-BIO) and dehydrated in a graded ethanol series. Thereafter, the samples were embedded in paraffin, cut into 4 µm thick sections, and stained with Modified Safranin O-Fast Green FCF cartilage Stain Kit (#G1371; Solarbio) according to the manufacturer's instructions. Immunohistochemistry staining was performed using antibodies against Collagen II (ab108349, Abcam; 1:200), Aggrecan (ab313636, Abcam; 1:2000), MMP13 (18165-1-AP, Protentech; 1:200), Collagen I (14695-1-AP, Proteintech; 1:500), IL-1β (16806-1-AP, Proteintech; 1:200), Immunofluorescence was performed using antibody against firefly luciferase (Firefly luciferase, Santa Cruz Biotechnology, sc-57603, 1:50). The Osteoarthritis Research Society International (OARSI) scoring system was conducted by two blinded observers for histological assessment. In addition, hematoxylin and eosin (H&E) staining for the heart, liver, spleen, lung, and kidney was performed to evaluate the toxicity of rhFGF18 mRNA-PL15 in animals.

RNA-seq and Analysis: Total RNA was extracted from human primary chondrocytes after stimulation with control CM or rhFGF18 mRNA CM for 24 h using FastPure Cell/Tissue Total RNA Isolation Kit V2 (Vazyme). 400 ng total RNA was used for the following library preparation. The poly(A) mRNA isolation was performed using Oligo(dT) beads. The mRNA fragmentation was performed using divalent cations and high temperatures. Priming was performed using Random Primers. First-strand cDNA and the second-strand cDNA were synthesized. The purified double-stranded cDNA was then treated to repair both ends and add a dA-tailing in one reaction, followed by a T-A ligation to add adaptors to both ends. Size selection of Adaptor-ligated DNA was then performed using DNA Clean Beads. Each sample was then amplified by PCR using P5 and P7 primers and the PCR products were validated. Then libraries with different indexes were multiplexed and loaded on an Illumina Novaseq instrument for sequencing using a 2×150 paired-end (PE) configuration according to the manufacturer's instructions. The reads were aligned to the human genome (hg38) using STAR v2.7.9a.[53] and gene expression levels were estimated using featureCounts.[54] DESeq2[55] was used to perform differential gene expression analysis. R package clusterProfiler was used to perform gene ontology (GO) and KEGG pathway analysis.[56] Heatmaps were generated by the pheatmap package.

Statistical Analysis: Unless otherwise stated, data were expressed as means ± SEM of the mean. For comparisons between two groups, means were compared using unpaired two-tailed Student's *t*-tests. Comparisons between multiple groups were performed by analysis of variance (ANOVA) followed by Bonferroni's posttest analysis. Sample size, including the number of mice per group, was chosen to ensure adequate power and was based on historical data. No exclusion criteria were applied for all analyses. All statistical analyses were performed using GraphPad Prism 8 software (GraphPad Software Inc.). $p < 0.05$ was considered statistically significant.

Supporting Information

Supporting Information is available from the Wiley Online Library or from the author.

Acknowledgements

M.S., B.M., and Z.P. contributed equally to this work. This study was funded by the Regional Innovation Joint Fund of the National Natural Science Foundation of China (Integrated Project) (U23A6009), Clinical Medicine Plus X-Young Scholars Project of Peking University (PKU2023LCXQ007), Beijing Natural Science Foundation (Z22022, JQ23029, L234024), the National Natural Science Foundation of China (HY2021-8, 82373807), Beijing Nova Program (20220484100, 20230484448), Beijing Municipal Science & Technology Commission (Z231100007223001, Z231100007223012), National Key Research and Development Program of China (2023YFC3405000), Emerging Engineering Interdisciplinary-Young Scholars Project, Peking University, the Fundamental Research Funds for the Central Universities (PKU2023XGK011).

Conflict of Interest

The authors declare no conflict of interest.

Data Availability Statement

The data that support the findings of this study are available from the corresponding author upon reasonable request.

© 2024 The Author(s). Advanced Healthcare Materials published by Wiley-VCH GmbH

Keywords

lipid nanoparticles, mRNA, osteoarthritis, recombinant human FGF18

Received: March 1, 2024
Revised: July 8, 2024
Published online: October 4, 2024

[1] D. J. Hunter, S. Bierma-Zeinstra, *Lancet* **2019**, *393*, 1745.
[2] I. J. Wallace, S. Worthington, D. T. Felson, R. D. Jurmain, K. T. Wren, H. Maijanen, R. J. Woods, D. E. Lieberman, *Proc. Natl. Acad. Sci.* **2017**, *114*, 9332.
[3] S. Safiri, A.-A. Kolahi, E. Smith, C. Hill, D. Bettampadi, M. A. Mansournia, D. Hoy, A. Ashrafi-Asgarabad, M. Sepidarkish, A. Almasi-Hashiani, G. Collins, J. Kaufman, M. Qorbani, M. Moradi-Lakeh, A. D. Woolf, F. Guillemin, L. March, M. Cross, *Ann. Rheum. Dis.* **2020**, *79*, 819.
[4] A. Latourte, M. Kloppenburg, P. Richette, *Nat Rev Rheumatol* **2020**, *16*, 673.
[5] L. Dai, X. Zhang, X. Hu, Q. Liu, Z. Man, H. Huang, Q. Meng, C. Zhou, Y. Ao, *Mol. Ther.* **2015**, *23*, 1331.
[6] Y. Xie, A. Zinkle, L. Chen, M. Mohammadi, *Nat. Rev. Rheumatol.* **2020**, *16*, 547.
[7] J S. Rockel, C. Yu, H. Whetstone, A M. Craft, K. Reilly, H. Ma, H. Tsushima, V. Puviindran, M. Al-Jazrawe, G M. Keller, B A. Alman, *J. Clin. Investig.* **2016**, *126*, 1649.
[8] J. L. Ellsworth, J. Berry, T. Bukowski, J. Claus, A. Feldhaus, S. Holderman, M. S. Holdren, K. D. Lum, E. E. Moore, F. Raymond, H. Ren, P. Shea, C. Sprecher, H. Storey, D. L. Thompson, K. Waggie, L. Yao, R. J. Fernandes, D. R. Eyre, S. D. Hughes, *Osteoarthr. Cartil.* **2002**, *10*, 308.
[9] E. E. Moore, A. M. Bendele, D. L. Thompson, A. Littau, K. S. Waggie, B. Reardon, J. L. Ellsworth, *Osteoarthr Cartil.* **2005**, *13*, 623.
[10] N. Zeng, X.-Y. Chen, Z.-P. Yan, J.-T. Li, T. Liao, G.-X. Ni, *Arthritis Res. Ther.* **2021**, *23*, 107.
[11] U. Sahin, K. Karikó, Ö. Türeci, *Nat. Rev. Drug Discovery* **2014**, *13*, 759.
[12] W. Zhao, X. Hou, O. G. Vick, Y. Dong, *Biomaterials* **2019**, *217*, 119291.
[13] R. J. Chandler, *Proc. Natl. Acad. Sci.* **2019**, *116*, 20804.
[14] S. Bartesaghi, K. Wallenius, D. Hovdal, M. Liljeblad, S. Wallin, N. Dekker, L. Barlind, N. Davies, F. Seeliger, M. S. Winzell, S. Patel, M. Theisen, L. Brito, N. Bergenhem, S. andersson, X. R. Peng, *Mol. Ther. – Nucleic Acids* **2022**, *28*, 500.
[15] A. M. Reichmuth, M. A. Oberli, A. Jaklenec, R. Langer, D. Blankschtein, *Ther. Deliv.* **2016**, *7*, 319.
[16] S. Qin, X. Tang, Y. Chen, K. Chen, Na Fan, W. Xiao, Q. Zheng, G. Li, Y. Teng, M. Wu, X. Song, *Signal Transduct. Target. Ther.* **2022**, *7*, 166.
[17] N. Chaudhary, D. Weissman, K. A. Whitehead, *Nat. Rev. Drug Discovery* **2021**, *20*, 817.
[18] P. S. Kowalski, A. Rudra, L. Miao, D. G. Anderson, *Mol. Ther.* **2019**, *27*, 710.
[19] J. Chen, Y. Xu, M. Zhou, S. Xu, A. J. Varley, A. Golubovic, R X Ze Lu, K. C. Wang, M. Yeganeh, D. Vosoughi, B. Li, *Proc. Natl. Acad. Sci.* **2023**, *120*, e2309472120.
[20] J. Yu, Q. Li, S. Luo, X. Wang, Q. Cheng, R. Hu, *bioRxiv* **2024**, 575299.
[21] Q. Cheng, T. Wei, L. Farbiak, L. T. Johnson, S. A. Dilliard, D. J. Siegwart, *Nat. Nanotechnol.* **2020**, *15*, 313.
[22] X. Wei, B. Shao, Z. He, T. Ye, M. Luo, Y. Sang, X. Liang, W. Wang, S. Luo, S. Yang, S. Zhang, C. Gong, M. Gou, H. Deng, Y. Zhao, H. Yang, S. Deng, C. Zhao, Li Yang, Z. Qian, J. Li, X. Sun, J. Han, C. Jiang, M. Wu, Z. Zhang, *Cell Res.* **2015**, *25*, 237.
[23] H. Zhou, Z. Zhang, Y. Mu, H. Yao, Y. Zhang, D.-A. Wang, *ACS Nano* **2024**, *18*, 10667.
[24] T. Suzuki, Y. Suzuki, T. Hihara, K. Kubara, K. Kondo, K. Hyodo, K. Yamazaki, T. Ishida, H. Ishihara, *Int. J. Pharm.* **2020**, *588*, 119792.
[25] A. Gigout, H. Guehring, D. Froemel, A. Meurer, C. Ladel, D. Reker, A. C. Bay-Jensen, M. A. Karsdal, S. Lindemann, *Osteoarthr. Cartil.* **2017**, *25*, 1858.
[26] Y. Jouan, Z. Bouchemla, B. Bardèche-Trystram, J. Sana, C. Andrique, H.-K. Ea, P. Richette, A. Latourte, M. Cohen-Solal, E. Hay, *Sci. Adv.* **2022**, *8*, eabn3106.
[27] H. Wu, Z. Peng, Y. Xu, Z. Sheng, Y. Liu, Y. Liao, Y. Wang, Ya Wen, J. Yi, C. Xie, X. Chen, J. Hu, B. Yan, H. Wang, X. Yao, W. Fu, H. Ouyang, *Stem Cell Res. Ther.* **2022**, *13*, 19.
[28] W. Hu, Y. Chen, C. Dou, S. Dong, *Ann. Rheum. Dis.* **2021**, *80*, 413.
[29] G. Zhen, C. Wen, X. Jia, Yu Li, J. L. Crane, S. C. Mears, F. B. Askin, F. J. Frassica, W. Chang, J. Yao, J. A. Carrino, A. Cosgarea, D. Artemov, Q. Chen, Z. Zhao, X. Zhou, L. Riley, P. Sponseller, M. Wan, W. W. Lu, Xu Cao, *Nat. Med.* **2013**, *19*, 704.
[30] P. G. Mitchell, H. A. Magna, L. M. Reeves, L. L. Lopresti-Morrow, S. A. Yocum, P. J. Rosner, K. F. Geoghegan, J. E. Hambor, *J. Clin. Investig.* **1996**, *97*, 761.
[31] D. Prieto-Alhambra, A. Judge, M. K. Javaid, C. Cooper, A. Diez-Perez, N. K. Arden, *Ann. Rheum. Dis.* **2014**, *73*, 1659.
[32] D. J. Hunter, D. Schofield, E. Callander, *Nat. Rev. Rheumatol.* **2014**, *10*, 437.
[33] S. L. Kolasinski, T. Neogi, M. C. Hochberg, C. Oatis, G. Guyatt, J. Block, L. Callahan, C. Copenhaver, C. Dodge, D. Felson, K. Gellar, W. F. Harvey, G. Hawker, E. Herzig, C. K. Kwoh, A. E. Nelson, J. Samuels, C. Scanzello, D. White, B. Wise, R. D. Altman, D. DiRenzo, J. Fontanarosa, G. Giradi, M. Ishimori, D. Misra, A. A. Shah, A. K. Shmagel, L. M. Thoma, M. Turgunbaev, et al., *Arthritis Rheumatol.* **2020**, *72*, 220.
[34] R. R. Bannuru, M. C. Osani, E. E. Vaysbrot, N. K. Arden, K. Bennell, S. M. A. Bierma-Zeinstra, V. B. Kraus, L. S. Lohmander, J. H. Abbott, M. Bhandari, F. J. Blanco, R. Espinosa, I. K. Haugen, J. Lin, L. A. Mandl, E. Moilanen, N. Nakamura, L. Snyder-Mackler, T. Trojian, M. Underwood, T. E. McAlindon, *Osteoarthr. Cartil.* **2019**, *27*, 1578.
[35] Y. Mori, T. Saito, S. H. Chang, H. Kobayashi, C. H. Ladel, H. Guehring, U. Chung, H. Kawaguchi, *J. Biol. Chem.* **2014**, *289*, 10192.
[36] D. Reker, C. F. Kjelgaard-Petersen, A. S. Siebuhr, M. Michaelis, A. Gigout, M. A. Karsdal, C. Ladel, A. C. Bay-Jensen, *J. Transl. Med.* **2017**, *15*, 250.
[37] A. Maroudas, *J. Anat.* **1976**, *122*, 335.
[38] E. Rohner, R. Yang, K. S. Foo, A. Goedel, K. R. Chien, *Nat. Biotechnol.* **2022**, *40*, 1586.
[39] A. G. Bajpayee, A. J. Grodzinsky, *Nat. Rev. Rheumatol.* **2017**, *13*, 183.
[40] C. H. Evans, V. B. Kraus, L. A. Setton, *Nat. Rev. Rheumatol.* **2014**, *10*, 11.
[41] C. Larsen, J. Østergaard, S. W. Larsen, H. Jensen, S. Jacobsen, C. Lindegaard, P. H. Andersen, *J. Pharm. Sci.* **2008**, *97*, 4622.
[42] S. Byun, Y. L. Sinskey, Y. C. S. Lu, T. Ort, K. Kavalkovich, P. Sivakumar, E. B. Hunziker, E. H. Frank, A. J. Grodzinsky, *Arch. Biochem. Biophys.* **2013**, *532*, 15.
[43] M. H. Y. Cheng, J. Leung, Y. Zhang, C. Strong, G. Basha, A. Momeni, Y. Chen, E. Jan, A. Abdolahzadeh, X. Wang, J A. Kulkarni, D. Witzigmann, P R. Cullis, *Adv. Mater.* **2023**, *35*, 2303370.
[44] X. Hou, T. Zaks, R. Langer, Y. Dong, *Nat. Rev. Mater.* **2021**, *6*, 1078.
[45] L. Zangi, K. O. Lui, A. von Gise, Q. Ma, W. Ebina, L. M. Ptaszek, D. Später, H. Xu, M. Tabebordbar, R. Gorbatov, B. Sena, M. Nahrendorf, D. M. Briscoe, R. A. Li, A. J. Wagers, D. J. Rossi, W. T. Pu, K. R. Chien, *Nat. Biotechnol.* **2013**, *31*, 898.
[46] S. Patel, R. C. Ryals, K. K. Weller, M. E. Pennesi, G. Sahay, *J. Controlled Release* **2019**, *303*, 91.

© 2024 The Author(s). Advanced Healthcare Materials published by Wiley-VCH GmbH

[47] J. F. Nabhan, K. M. Wood, V. P. Rao, J. Morin, S. Bhamidipaty, T. P. LaBranche, R. L. Gooch, F. Bozal, C. E. Bulawa, B. C. Guild, *Sci. Rep.* **2016**, *6*, 20019.
[48] M. Chen, Y. Lu, Y. Liu, Q. Liu, S. Deng, Y. Liu, X. Cui, J. Liang, X. Zhang, Y. Fan, Q. Wang, *Adv. Mater.* **2024**, *36*, 2312559.
[49] J. M. Hollander, A. Goraltchouk, J. Liu, E. Xu, F. Luppino, T. E. McAlindon, L. Zeng, A. Seregin, *Curr. Gene Ther.* **2024**, *24*, 331.
[50] S. Sieber, A. Gigout, *Exp. Cell Res.* **2020**, *395*, 112236.
[51] Z. Song, Y. Li, C. Shang, G. Shang, H. Kou, J. Li, S. Chen, H. Liu, *Front. Cell Dev. Biol.* **2021**, *9*, 786546.
[52] N. Vostrosablin, S. Lim, P. Gopal, K. Brazdilova, S. Parajuli, X. Wei, A. Gromek, D. Prihoda, M. Spale, A. Muzdalo, J. Greig, C. Yeo, J. Wardyn, P. Mejzlik, B. Henry, A. W. Partridge, D. A. Bitton, *NAR Genom. Bioinform.* **2024**, *6*, lqae028.
[53] A. Dobin, C. A. Davis, F. Schlesinger, J. Drenkow, C. Zaleski, S. Jha, P. Batut, M. Chaisson, T. R. Gingeras, *Bioinformatics* **2013**, *29*, 15.
[54] P. Ewels, M. Magnusson, S. Lundin, M. Käller, *Bioinformatics* **2016**, *32*, 3047.
[55] M. I. Love, W. Huber, S. Anders, *Genome Biol.* **2014**, *15*, 550.
[56] T. Wu, E. Hu, S. Xu, M. Chen, P. Guo, Z. Dai, T. Feng, L. Zhou, W. Tang, L. Zhan, fu, S. Liu, X. Bo, G. Yu, *Innov.* **2021**, *2*, 100141.

© 2024 The Author(s). Advanced Healthcare Materials published by Wiley-VCH GmbH